Designing magnetic field sensor based on tapered photonic crystal fibre assisted by a ferrofluid

Mostafa Taghizadeh[1,*] **and Forough Bozorgzadeh**[2]

[1] Atomic and molecular group, Faculty of Physics, Yazd University, Yazd, Iran
[2] Faculty of Physics, University of Tabriz, Tabriz, Iran

ABSTRACT

A novel magnetic field sensor is proposed based on the combination of in-line tapered photonic crystal fibre (PCF) Mach-Zehnder interferometer (MZI) and magnetic nanoparticles. The sensor was theoretically investigated and experimentally realized. The effect of the mechanical strain and the magnetic field on the sensitivity of the sensor is studied. It is found that the proposed sensor shows a strain sensitivity of $1\text{pm}/\mu\varepsilon$. In order to evaluate the magnetic nanoparticles effect on the intensity of output light, the sensitivity response of the device has been measured under different magnetic field strengths for three length scales. The experimental results show refractive index changes of the magnetic nanoparticles-infiltrated PCF - acting as a fibre cladding - under applied magnetic field leads to variations of the interferometric output. The sensitivity of magnetic field measurement could reach up to 0.003 dB/mT. The results show a very good linear response that is an essential requirement for the practical sensors. The proposed magnetic field sensor finds applications in various areas, such as optical sensing, military, power industry, and tunable photonic devices.

1 Introduction

Photonic crystal fibres (PCFs), first invented and demonstrated in 1996[1], have peculiar properties owing to the complex pattern of air-holes in their cross-section that runs along the fibre. The intrinsic air-holes of the PCF cladding that can be infiltrated by gases, dyes, liquids, or low-viscosity polymers[2,3], establish an adaptable platform for developing tunable opto-fluidic devices. For example, a tunable electro-optical modulator has been realized by filling one air-hole of PCF with liquid-crystal[4]. Also, it is shown that the infiltration of opto-fluids into the first ring of the PCF cladding may lead to the dispersion engineering for tunable wavelength conversion[5]. The temperature and refractive index sensors based on in-line Fabry–Pérot interferometer in PCF is reported[6]. It is shown that the sensitivity can be increased via optimizing the length of PCF. Tapered PCF is employed in an interferometer structure to construct a miniaturized refractive index sensor[7]. Using the advantages of polarization-maintaining PCFs, a magnetic field sensor with the sensitivity of 242 pm/mT is reported[8].

With the advent of nanotechnology, a new class of smart nano-materials emerge as a promising platform for novel optoelectronic devices. In particular, ferrofluids (FFs) or magnetic fluids, which are stable colloidal solutions containing surfactant-coated magnetic nanoparticles dispersed in an appropriate liquid, possess both the magnetism of magnetic nanoparticles and fluidity of liquid materials[9,10]. The unique properties of FFs, such as optical anisotropy and birefringence, Faraday effect, tunable refractive index, and field-dependent transmission, can be tuned by external magnetic fields. Due to these outstanding magneto-optical properties, FFs has been used to design unique photonic devices, such as optical switches[11], optical modulators[12], tunable optical filters[13], optical fibre gratings[14] and sensors[15,16].

Accurate measurements of magnetic field is of scientific and industrial importance for many applications such as medicine, military, vehicle monitoring and geological prospecting. In the last few decades, various types of magnetic field sensor are proposed and realized, for example based on side-polished fiber[17], cascaded microfiber coupler[18], fibre ring cavity laser[19], tapered microfiber[20], and birefringence in liquid core optical waveguide[21]. The sensitivity response of the magnetic field sensors had reported in terms of changes in wavelength shift or output intensity. Among different kinds of magnetic field sensors, fiber-optic interferometric sensors are the one that have attracted a great deal of research attention due to the compactness, immunity to electromagnetic interference, low-cost and easy fabrication. A fibre-optic interferometer operates based on the interference between two propagating beams either in two different adjacent fibres or through different optical paths in a single optical fibre. Especially, the unique properties of PCFs makes them appealing for optical sensing. PCF-based interferometric sensors include Fabry–Pérot interferometer, Mach-Zehnder interferometer, Michelson interferometer and Sagnac interferometer[22–24]. In particular, to implement an in-line Mach-Zehnder interferometer (MZI), a beam splitter and a beam combiner are needed to guide light in the arms of the interferometer[25]. Generally, an in-line fibre-based interferometer can be realized via core misalignment and collapsing methods. In these methods, a more complicated interference pattern is

expected due to the possibility of exciting the high-order cladding modes[26].
In this work, we report a low-cost highly-sensitive magnetic field sensor using the advantages of an in-line MZI in a FF-assisted tapered PCF. The sensor behaviour has been investigated both theoretically and experimentally. In the first step, the Fe_3O_4 magnetic nanoparticles are synthesized using a reverse co-precipitation method. Then, the by injecting a small amount of the FF into the PCF air-holes and exposing the PCF-MZI to the magnetic field, the refractive index variations is verified. Thus, magnetically-tunable refractive index can lead to the changes in output light. The PCF is then tapered using a custom made tapering machine. It is found that the proposed sensor shows a strain sensitivity of 1pm/$\mu\varepsilon$. For a given length of tapered-PCF, it is shown that the sensitivity of sensor depend on the applied magnetic field. It is found that the sensitivity is strongly dependent on length of the MZI. We have shown that the magnetic field of few mT can be detected with higher sensitivity of 0.003 dB/mT. The results show a very good linear response that is an essential requirement for the practical sensors.

2 Materials and methods

2.1 Synthesis of Fe_3O_4 magnetic nanoparticle

Fe_3O_4 magnetic nanoparticles of average size $\sim 12-15$ nm were synthesized using the reverse co-precipitation method which is an efficient low-cost method. All chemicals used in the experiment were purchased from Sigma-Aldrich. In the synthesis, the base solution is prepared by diluting 30% Ammonia (NH_4OH) with adding doubled distilled water (DDW) (3:2 ratio) in a three-neck flask. The solution is mechanically stirred and heated to 80 °C under argon. Then, Fe salt solution is prepared by dissolving ferrous sulfate heptahydrate ($FeSO_4 \cdot 7H_2O$) and $Fe(NO_3)_3$ (with 1:2 molar ratio) in 200 ml DDW. While keeping the temperature constant at 80 °C, these solutions were mixed together under vigorous stirring for 30 min under argon. The final solution was turned from brown to black indicating the nucleation and growth of magnetic nanoparticles. After rapidly cooled down to room temperature using an ice bath, the solution is carefully injected inside the PCF air-holes using a syringe with a 0.5 mm diameter needle. The FF-infiltrated PCF has been left for 24 h before any further steps.

2.2 Fabrication and Sensing Principle

The experimental setup of the magnetic field sensor is shown in Figure 1(a). The sensor structure consists of a broadband light source (BLS) (Thorlabs, SLS202(/M)), a sensing PCF-based interferometer, an optical spectrum analyser (OSA) (Yokogawa, AQ6370D). As shown in Figure 1(b), to implement the in-line PCF-MZI, a small section of PCF is spliced between a lead-in and a lead-out standard SMF-28 fibre. The PCF used in this experiment is a large-mode-area PCF (Thorlabs, LMA-35) which has a core diameter of 35μm, outer cladding diameter of 335μm and the attenuation of < 0.01 dB/m 1550 nm. The fusion splicing is performed with a commercial fusion splicing machine (Ericsson FSU-955). The length of the collapsed zones is carefully controlled via changing the intensity and the duration of arc discharge. In the fabricated PCF-MZI, one propagating beam is referred to the sensing arm and the other one is called reference arm[23]. Even though the physical length of the two arms is identical, the interference signal can be detected. Physically, this behaviour can be understood from the fact that since the effective indices of the core and cladding are not identical, there will be an optical path difference between the arms of the interferometer. In this case, the phase velocity of the reference and sensing arm is different.
Since the MZI-based sensors are very sensitive to fibre bending, the device was firmly kept constant with the aid of fibre holders. In order to apply the axial strain, the two sides of inline PCF-MZI were clamped to two stages: a fibre holder of micro-positioner stage and a fibre holder of fixed stage. The PCF-MZI is then placed between two poles of an electromagnet, which generates a uniform magnetic field. The intensity of magnetic field can be adjusted by tuning the power supply. The magnetic field direction is perpendicular to the propagation of light and the optical fibre axis. The operating principle of the sensor is as follows: Light from the BLS is coupled into the lead-in SMF, and enters the collapsed zone of the PCF. In this region, light promptly begins to diffract, leading to mode broadening. Then it passes through the PCF region, recombines at the second collapsed zone. The output light is monitored and analysed by the OSA with the wavelength resolution 0.02 nm. The occurrence of total internal reflection and more importantly the interference between core and cladding modes is dependent on the axial strain, strength of magnetic field and the length of the MZI.
The device can be modelled using a core and cladding mode interference equation given by[26]

$$I_{\text{out}} = I_1 + I_2 + 2\sqrt{I_1 I_2}\cos(\Delta\Phi), \tag{1}$$

where I_{out} is the intensity of the total interference signal, I_1 and I_2 are the intensities of light propagating in the fibre core and cladding. $\Delta\Phi$ is the phase difference between the core and cladding modes

$$\Delta\varphi = \frac{2\pi}{\lambda}\Delta n_{\text{eff}}(\lambda)\, L, \tag{2}$$

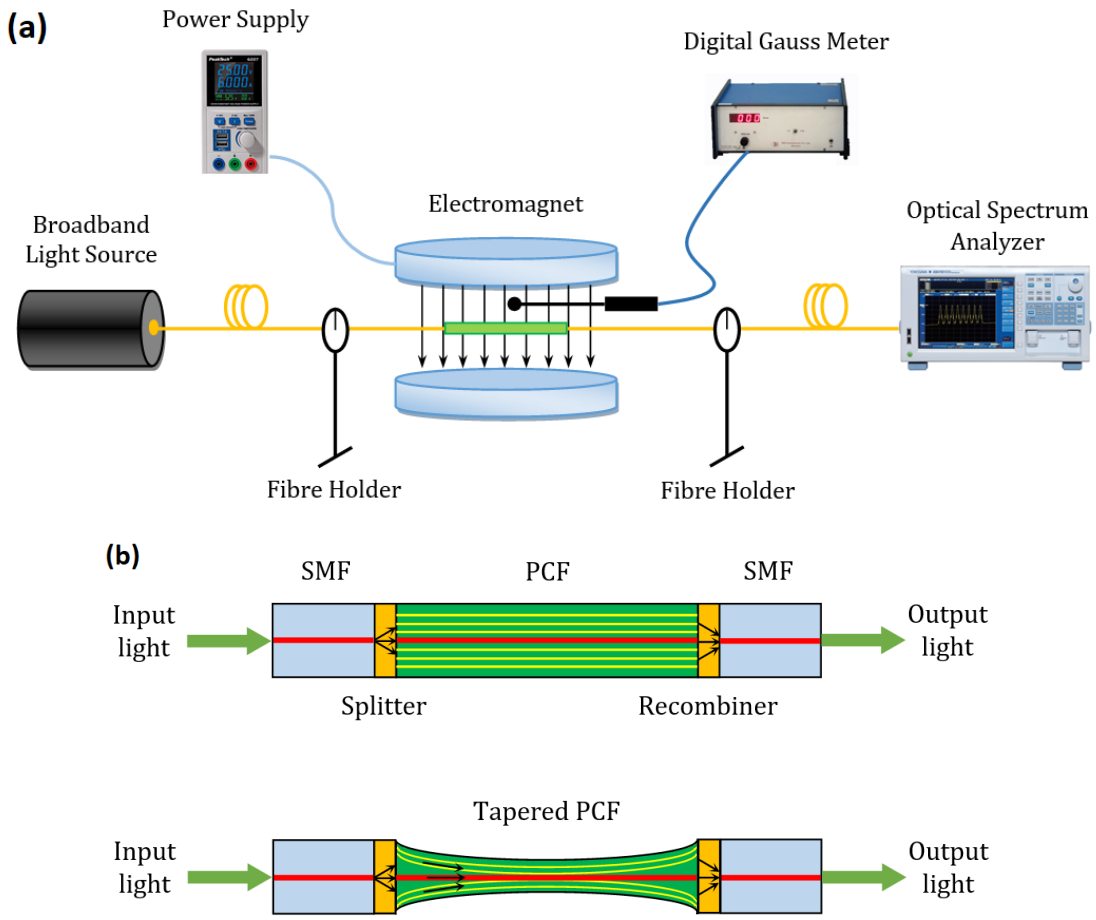

Figure 1. Schematic diagram of (a) the experimental setup for magnetic field sensing, (b) the in-line Mach- Zehnder interferometer in tapered PCF.

where $\Delta n_{\text{eff}} = n_{\text{eff}}^{\text{core}} - n_{\text{eff}}^{\text{clad}}$ is the effective refractive index difference between the core and cladding, L is the length of interferometer and λ is the central wavelength of the BLS. The minimum in the intensity of the output spectrum will occur when $\lambda_{\text{min}} = 2\Delta n_{\text{eff}} L/(2\text{m}+1)$, where m is the interference order.

3 Experimental Results and Discussion

In this section, the main results are presented and the effect of strain and magnetic field on the intensity of output light is investigated. Figure 2(a) shows the fundamental core mode of the PCF. The simulations were carried out using commercial software (ANSYS Lumerical 2020). Transmission spectrum the PCF-MZI in the absence of an external magnetic field is presented in Figure 2(b). It can be realized that the intensity dip is very narrow and the insertion loss is small around the central wavelength. This intensity dip can be shifted with changing the length of PCF. The theoretical result shows a very good agreement with the results obtained from experiment.

Figure 3(a) shows the axial strain response of the in-line PCF-MZI sensor. From the transmission spectrum of the PCF-MZI, it can be observed that the intensity dip is blue-shifted without a significant change in its shape as the axial strain is increased from 0 to 600 $\mu\varepsilon$. In fact, the changes of fibre dimensions and the photo-elastic effect of the fibre due to the applied axial strain leads to a shift in interferometric spectrum. At a constant temperature, the wavelength shift due to the strain can be expressed as $\Delta\lambda/\lambda = -(1+2\nu+p_e)\,\varepsilon$, where ν is the Poisson ratio of the fibre, p_e is the effective strain-optic coefficient, and $\varepsilon = \Delta L/L$ is the axial strain applied on the fibre[27]. The relationship between the applied strain and the dip wavelength is presented in Figure 3(b). A fitting curve of the experimental data shows that the wavelength shift is linear with the correlation factor of $R^2 = 0.99$. The wavelength of intensity dip shifts from 1549.8 nm to1548.9 nm, and the strain sensitivity is found to be 1 pm/$\mu\varepsilon$.

As mentioned before, the proposed sensor operates based on light intensity modulation. It is well-known that the refractive

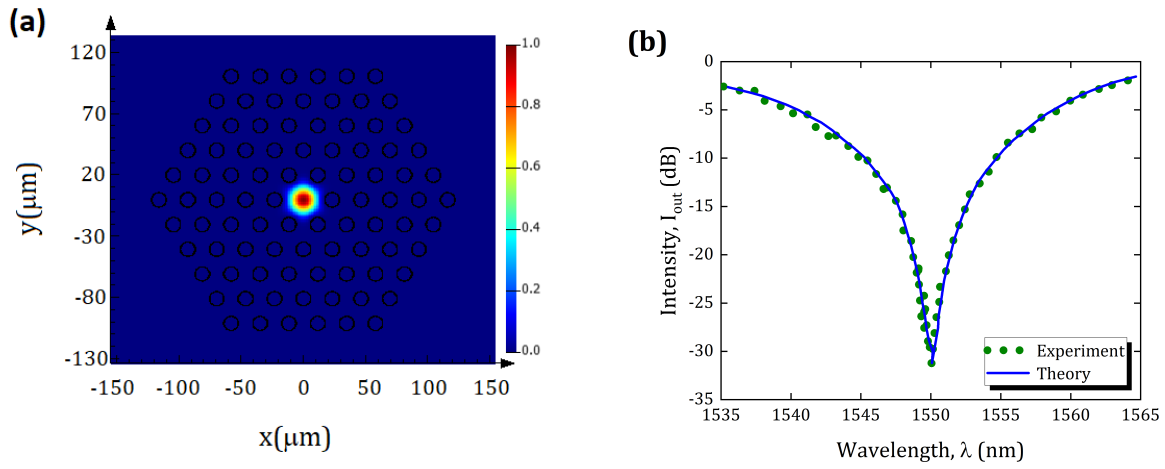

Figure 2. (a) Calculated field distributions of PCF core mode at 1550 nm wavelength, (b) the output intensity of PCF-MZI as a functions of wavelength.

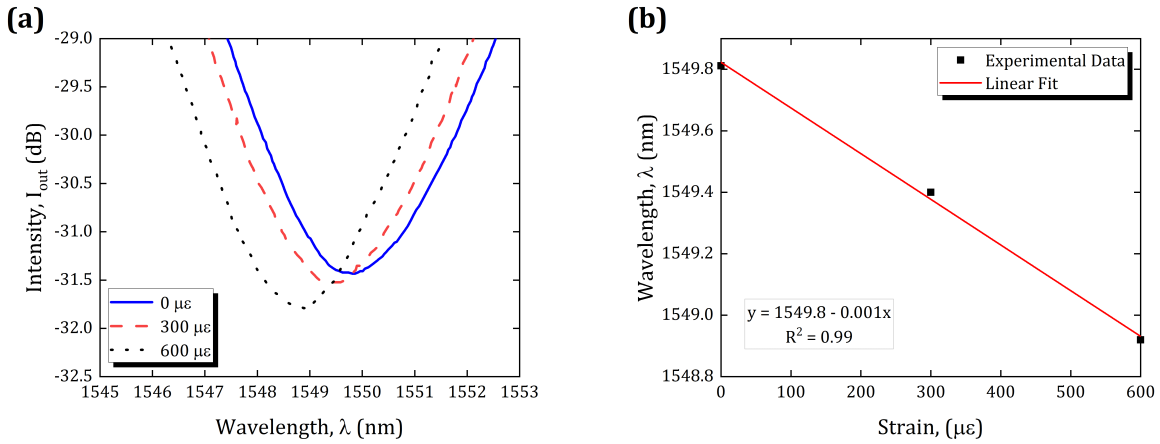

Figure 3. (a) The output intensity of PCF-MZI as a functions of wavelength, (b) The wavelength shift as a function of the axial strain.

index of PCF background material (i.e. pure silica) is not sensitive to magnetic field. However, the randomly homogenous structure of FFs changes under an external magnetic field. Therefore, field-dependent rearrangement of Fe_3O_4 nanoparticles leads to the refractive index variation of the FF, accordingly the light modulation is possible. The relationship between refractive index and magnetic field for Fe_3O_4 FF has been extensively reported in the literature[28,29], and it is found that the refractive index of magnetic fluid increases with enhancing field strength[30]. Figure 4 shows the variation of intensity dip as a function of magnetic field strength. The effect of magnetic field strength on the output light intensity is investigated by gradually increasing the applied magnetic field from 0 to 140 mT. The magnetic field dependence of the intensity dip is obtained for three different lengths of PCF-MZI. The dip intensity of output light is an ascending function of the applied magnetic field. The experimental results show that the sensitivity of magnetic field measurement could reach 0.021 dBm/mT, 0.024 dBm/mT and 0.003 dBm/mTfor the PCF-MZI length of $L = 30$ mm, $L = 40$ mm and $L = 50$ mm, respectively . From Figure 4(a), it can be predicted that the intensity of output light changes slightly for the magnetic field below 5 mT, which is in agreement with previous results[31]. It can be seen that the linear correlation is inversely proportional to the sensing length. It is worth to mention that the intensity of the output light tends to be constant for the magnetic strength range beyond the saturation magnetization of Fe_3O_4 magnetic nano-particles, which in not investigated in this study.

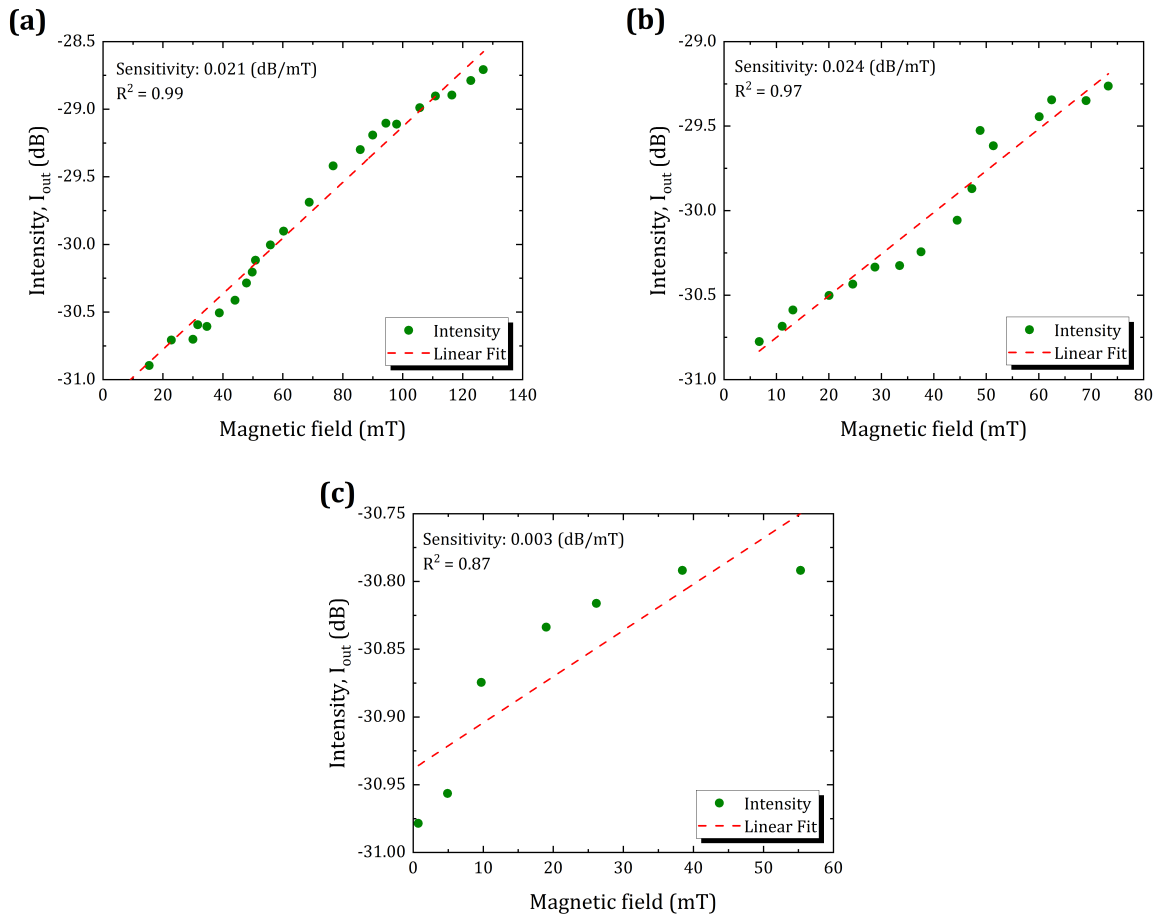

Figure 4. Measurements of the output intensity as a functions of magnetic field variation for (a) $L = 30$ mm, (b) $L = 40$ mmand (c) $L = 50$ mm.

4 Conclusion

In conclusion, we have demonstrated a highly-sensitive magnetic field sensor based on the combination of an in-line PCF-MZI with the characteristics of the magnetic nanoparticles. First, the Fe_3O_4 ferrofluid was synthesized using the reverse co-precipitation method. Then, by infiltrating air-holes of the PCF with FF and fusion splicing with standard SMFs, in-line PCF-MZI is realized. The effect of the mechanical strain and the magnetic field on the sensitivity of sensor is studied. It is found that the proposed sensor shows a strain sensitivity of 1 pm/$\mu\varepsilon$. The experimental results show refractive index variations of the FF-filled PCF under applied magnetic field leads tochanges of the interferometric output. The sensitivity of magnetic field measurement could reach up to 0.003 dB/mT. The results show a very good linear response that is an essential requirement for the practical sensors. The proposed magnetic field sensor finds applications in various areas, such as optical sensing, military, power industry, and tunable photonic devices.

Disclosure statement

The authors declare no conflict of interest.

Author contributions statement

M.T. provided the idea and designed the experiments, F.B. analysed the data and wrote the manuscript. All authors discussed the results and contributed to the manuscript.

Author information

Mostafa Taghizadeh: e-mail: mostafa.taghizadeh@hotmail.com (corresponding author)
Forough Bozorgzadeh: https://orcid.org/0000-0002-2799-2754

References

1. Knight, J. C., Birks, T. A., Russell, P. S. J. & Atkin, D. M. All-silica single-mode optical fiber with photonic crystal cladding. *Opt. Lett.* **21**, 1547–1549, DOI: 10.1364/OL.21.001547 (1996).

2. Martelli, C. *et al.* Evanescent-field spectroscopy using structured optical fibers: Detection of charge-transfer at the porphyrin-silica interface. *J. Am. Chem. Soc.* **131**, 2925–2933, DOI: 10.1021/ja8081473 (2009). PMID: 19203267, https://doi.org/10.1021/ja8081473.

3. Markos, C., Vlachos, K. & Kakarantzas, G. Bending loss and thermo-optic effect of a hybrid pdms/silica photonic crystal fiber. *Opt. Express* **18**, 24344–24351, DOI: 10.1364/OE.18.024344 (2010).

4. Huang, Y. *et al.* Tunable electro-optical modulator based on a photonic crystal fiber selectively filled with liquid crystal. *J. Light. Technol.* **37**, 1903–1908, DOI: 10.1109/JLT.2019.2894910 (2019).

5. Pakarzadeh, H., Derakhshan, R. & Hosseinabadi, S. Tunable wavelength conversion based on optofluidic infiltrated photonic crystal fibers. *J. Nonlinear Opt. Phys. & Mater.* **28**, 1950002, DOI: 10.1142/S0218863519500024 (2019). https://doi.org/10.1142/S0218863519500024.

6. Dash, J. N. & Jha, R. Inline microcavity-based pcf interferometer for refractive index and temperature sensing. *IEEE Photonics Technol. Lett.* **27**, 1325–1328, DOI: 10.1109/LPT.2015.2421308 (2015).

7. Ahmed, F., Ahsani, V., Melo, L., Wild, P. & Jun, M. B. G. Miniaturized tapered photonic crystal fiber mach–zehnder interferometer for enhanced refractive index sensing. *IEEE Sensors J.* **16**, 8761–8766, DOI: 10.1109/JSEN.2016.2566663 (2016).

8. Thakur, H. V., Nalawade, S. M., Gupta, S., Kitture, R. & Kale, S. N. Photonic crystal fiber injected with fe3o4 nanofluid for magnetic field detection. *Appl. Phys. Lett.* **99**, 161101, DOI: 10.1063/1.3651490 (2011). https://doi.org/10.1063/1.3651490.

9. Gubin, S. P., Koksharov, Y. A., Khomutov, G. B. & Yurkov, G. Y. Magnetic nanoparticles: preparation, structure and properties. *Russ. Chem. Rev.* **74**, 489–520, DOI: 10.1070/RC2005v074n06ABEH000897 (2005).

10. Luo, L., Pu, S., Dong, S. & Tang, J. Fiber-optic magnetic field sensor using magnetic fluid as the cladding. *Sensors Actuators A: Phys.* **236**, 67 – 72, DOI: https://doi.org/10.1016/j.sna.2015.10.034 (2015).

11. Horng, H. E. *et al.* Tunable optical switch using magnetic fluids. *Appl. Phys. Lett.* **85**, 5592–5594, DOI: 10.1063/1.1833564 (2004). https://doi.org/10.1063/1.1833564.

12. Horng, H. E. *et al.* Designing optical-fiber modulators by using magnetic fluids. *Opt. Lett.* **30**, 543–545, DOI: 10.1364/OL.30.000543 (2005).

13. Liu, T. *et al.* Tunable magneto-optical wavelength filter of long-period fiber grating with magnetic fluids. *Appl. Phys. Lett.* **91**, 121116, DOI: 10.1063/1.2787970 (2007). https://doi.org/10.1063/1.2787970.

14. Candiani, A., Margulis, W., Sterner, C., Konstantaki, M. & Pissadakis, S. Phase-shifted bragg microstructured optical fiber gratings utilizing infiltrated ferrofluids. *Opt. Lett.* **36**, 2548–2550, DOI: 10.1364/OL.36.002548 (2011).

15. Zhao, Y., Liu, X., Lv, R.-Q., Zhang, Y.-N. & Wang, Q. Review on optical fiber sensors based on the refractive index tunability of ferrofluid. *J. Light. Technol.* **35**, 3406–3412 (2017).

16. Cennamo, N. *et al.* A magnetic field sensor based on spr-pof platforms and ferrofluids. *IEEE Transactions on Instrumentation Meas.* **70**, 1–10, DOI: 10.1109/TIM.2020.3035114 (2021).

17. Li, Y. *et al.* All-fiber-optic vector magnetic field sensor based on side-polished fiber and magnetic fluid. *Opt. Express* **27**, 35182–35188, DOI: 10.1364/OE.27.035182 (2019).

18. Mao, L. *et al.* Magnetic field sensor based on cascaded microfiber coupler with magnetic fluid. *J. Appl. Phys.* **120**, 093102, DOI: 10.1063/1.4962177 (2016). https://doi.org/10.1063/1.4962177.

19. Bai, X. *et al.* Magnetic field sensor using fiber ring cavity laser based on magnetic fluid. *IEEE Photonics Technol. Lett.* **28**, 115–118, DOI: 10.1109/LPT.2015.2487379 (2016).

20. Ma, Z. *et al.* A highly sensitive magnetic field sensor based on a tapered microfiber. *IEEE Photonics J.* **10**, 1–8, DOI: 10.1109/JPHOT.2018.2862949 (2018).

21. Wang, W., Zhang, H., Li, B., Li, Z. & Miao, Y. Optical fiber magnetic field sensor based on birefringence in liquid core optical waveguide. *Opt. Fiber Technol.* **50**, 114 – 117, DOI: https://doi.org/10.1016/j.yofte.2019.03.011 (2019).

22. Ding, W., Jiang, Y., Gao, R., Wang, Z. & Liu, Y. An in-line photonic crystal fibre-based mach–zehnder interferometer with temperature compensation. *Meas. Sci. Technol.* **25**, 107002, DOI: 10.1088/0957-0233/25/10/107002 (2014).

23. Hu, D. J. J., Wong, R. Y.-N. & Shum, P. P. Photonic Crystal Fiber–Based Interferometric Sensors. In *Selected Topics on Optical Fiber Technologies and Applications*, DOI: 10.5772/intechopen.70713 (InTech, 2018).

24. Shao, M., Sun, H., Liang, J., Han, L. & Feng, D. In-fiber michelson interferometer in photonic crystal fiber for humidity measurement. *IEEE Sensors J.* **21**, 1561–1567, DOI: 10.1109/JSEN.2020.3019717 (2021).

25. Wei, T., Lan, X., Zhang, Y. & Xiao, H. Fiber inline core-cladding-mode interferometer fabricated by CO2 laser irradiation. In Xiao, H., Fan, X. & Wang, A. (eds.) *Photonic Microdevices/Microstructures for Sensing*, vol. 7322, 7 – 11, DOI: 10.1117/12.818624. International Society for Optics and Photonics (SPIE, 2009).

26. Choi, H. Y., Kim, M. J. & Lee, B. H. All-fiber mach-zehnder type interferometers formed in photonic crystal fiber. *Opt. Express* **15**, 5711–5720, DOI: 10.1364/OE.15.005711 (2007).

27. Li, E. Temperature compensation of multimode-interference-based fiber devices. *Opt. Lett.* **32**, 2064–2066, DOI: 10.1364/OL.32.002064 (2007).

28. Yang, S. Y. *et al.* Magnetically-modulated refractive index of magnetic fluid films. *Appl. Phys. Lett.* **81**, 4931–4933, DOI: 10.1063/1.1531831 (2002). https://doi.org/10.1063/1.1531831.

29. Horng, H. E., Hong, C.-Y., Yang, S. Y. & Yang, H. C. Designing the refractive indices by using magnetic fluids. *Appl. Phys. Lett.* **82**, 2434–2436, DOI: 10.1063/1.1568147 (2003). https://doi.org/10.1063/1.1568147.

30. Chen, L. X., Huang, X. G., Zhu, J. H., Li, G. C. & Lan, S. Fiber magnetic-field sensor based on nanoparticle magnetic fluid and fresnel reflection. *Opt. Lett.* **36**, 2761–2763, DOI: 10.1364/OL.36.002761 (2011).

31. Miao, Y. *et al.* Magnetic field tunability of optical microfiber taper integrated with ferrofluid. *Opt. Express* **21**, 29914–29920, DOI: 10.1364/OE.21.029914 (2013).